NASA TECHNICAL MEMORANDUM

NASA TM X-2739

NASA TM X-2739

PERFORMANCE COMPARISON OF THREE NORMAL-SHOCK POSITION SENSORS FOR MIXED-COMPRESSION INLETS

by Miles O. Dustin and Gary L. Cole

Lewis Research Center

Cleveland, Ohio 44135

NATIONAL AERONAUTICS AND SPACE ADMINISTRATION • WASHINGTON, D. C. • MARCH 1973

PERFORMANCE COMPARISON OF THREE NORMAL-SHOCK POSITION SENSORS FOR MIXED-COMPRESSION INLETS

by Miles O. Dustin and Gary L. Cole

Lewis Research Center

SUMMARY

This report describes the performance of three types of normal shock position sensors tested in a two-dimensional, mixed-compression inlet designed for Mach 2.7. The three sensors used different logic means to implement the logic required to determine shock position. The first sensor used electronic logic with inputs provided by pressure transducers measuring the pressures from wall static pressure taps located in the cowl of the inlet in the vicinity of the throat. Two of these identical electronic sensors, one in the upper duct and one in the lower duct, were tested in the inlet. The second sensor used fluidic amplifiers connected to wall static pressure taps, and the third sensor used switches connected directly to wall static pressure taps. All three sensors had stepwise-continuous, electronic outputs proportional to shock position.

The criterion for determining the location of the shock in the inlet throat was the same for all three sensors. The three sensors were evaluated both statically and dynamically at the design Mach number of 2.7 and at Mach 2.3. The inlet angle of attack was varied from 0° to 3.35°. Test results show that the three types of sensors could be made to measure the correct steady-state shock position within two static taps of the correct position. The accuracy was not affected by angle of attack or off-design Mach number operation.

The dynamic response of these sensors was also evaluated for variations in shock position from 1 to 80 hertz. The lower duct electronic sensor dropped one level out of nine levels at 20 hertz. At 80 hertz four levels were omitted from its output. The upper duct electronic sensor maintained nine levels of output at 60 hertz. The fluidic sensor dropped two levels at 40 hertz and continued to indicate the remaining seven levels at 80 hertz. The sensor using the direct switches exhibited erratic operation over the entire frequency range. Operation could probably be improved by better switch design.

INTRODUCTION

To maintain high inlet performance, a mixed-compression inlet must operate with the normal shock as close to the throat as possible. If the shock moves downstream, the shock occurs at a higher Mach number resulting in larger losses across the shock and greater compressor face distortion. If the shock occurs too close to the throat, an airflow disturbance originating either upstream or downstream of the shock can cause the shock to move upstream of the throat resulting in an inlet unstart. Upstream disturbances can be caused by atmospheric turbulence, temperature gradients, or shocks from passing aircraft, while downstream disturbances can be created by changes in engine or bypass airflow. A shock position margin is therefore required to maintain inlet stability. The size of the margin depends on the capabilities of the normal shock control and the accuracy with which the normal shock position is known. Large margins, of course, result in low pressure recovery and high distortion.

Most supersonic inlet control systems use a duct static pressure downstream of the normal shock to infer shock position. The gain of this measurement is usually nonlinear, and the signal must be biased to compensate for inaccuracies due to operating at off-design Mach numbers, altitudes, angles of attack, and yaw angles. An alternate approach is to measure the shock position directly (refs. 1 to 5). The present effort is this latter concept wherein the measurement of the normal shock position is deduced from wall static pressure profiles in the vicinity of the shock.

For inlets with internal compression the ideal static pressure profile occurs as shown in figure 1. The minimum supersonic flow Mach number occurs at the inlet throat. Downstream of the throat the Mach number increases and static pressure decreases as area increases. At the normal shock there is a discontinuous rise in pressure. Downstream of the shock the pressure continues to rise, since the flow is subsonic and the area continues to increase.

In actual practice the pressure profile is not as ideal as in figure 1. Figure 2 shows typical cowl-wall static pressure profiles for a mixed-compression inlet as measured by a series of closely spaced static pressure taps. Curves for three different shock positions are shown. Each profile was obtained with the location of the leading edge of the shock as noted on the figure. The nonideal nature of the profiles is due to such things as shock-boundary-layer interactions, oblique shock reflections, and a finite shock train length. Although the pressure rise across the shock is not discontinuous as in the ideal case, there is a large pressure gradient in the vicinity of the shock. This gradient may be used for determining shock position.

The location of the normal shock may be inferred by determining the lowest point in the wall static pressure profile. This point would be a short distance upstream of the shock pressure rise. One scheme using fluidic components for implementing the required logic is reported in reference 1. Another used electronic components for the

same logic scheme as reported in reference 2. Both of these sensors were evaluated in an axisymmetric mixed-compression inlet with a translating centerbody. Tests were run only at zero angle of attack and design Mach number. In a later study at Lewis, reported in reference 3, it was found that the shape of the wall static pressure profile is altered by angle of attack. The criterion used in references 1 and 2, therefore, is valid only at zero angle of attack and is not practical for a flight inlet system. The study of reference 3 concluded that the most practical criterion was to compare the individual wall static pressures with a suitably chosen reference pressure. For the particular value of reference pressure used in reference 3, the actual shock was found to be within one or two taps upstream of where the static tap location becomes greater than the reference pressure. Other shock sensors which used variations of this criterion are reported in references 4 and 5.

This report presents the results of a program that evaluates the performance of three types of shock position sensors using the criteria developed in reference 3. Three different means were used to implement the same logic: (1) electronic logic using pressure transducers, (2) fluidic logic actuating electric output pressure switches, and (3) electric output pressure switches alone connected directly to wall static taps. The three sensors were evaluated in the Lewis 10- by 10-Foot Supersonic Wind Tunnel. Both static and dynamic tests were run.

SYMBOLS

A, B, C, D, E, F, G, H	throat static-pressure taps (fig. 11)
M	Mach number
O_1, O_2	outputs of fluidic amplifiers
P_{th}	throat total pressure, N/cm^2
p	static pressure, N/cm^2
S	outputs of shock sensors
α	angle of attack, deg
Subscripts:	
A, B, C, D, E, F, G, H	pressure taps
US	upstream of tap A

SENSOR DESCRIPTION

General

Three normal shock position sensors were built and tested in a mixed-compression, two-dimensional ramp inlet at Mach 2.7 and 2.3 through 3.35^{o} of angle of attack. The three sensors all used the same criterion for determining the shock location from the cowl wall static pressure profile. The profile is measured by a row of closely spaced pressure taps near the inlet throat. The criterion is that if the pressure from a particular tap is greater than a certain reference pressure and the adjacent upstream tap has a pressure lower than the reference pressure, the leading edge of the shock is indicated between these two taps. The reference pressure was chosen as a fixed fraction of the inlet throat total pressure to make the sensor insensitive to altitude.

Figure 3 illustrates the operation principle of the sensors. The cowl-wall static pressure is plotted as a function of distance from the cowl lip for three different shock positions. The tap locations (A to H) are noted on the distance axis. The reference pressure is shown as a fixed fraction of the throat total pressure. For the purpose of this test, the reference pressure was selected to be 0.528 times the throat pressure. In choosing this reference pressure value it was assumed that regions in which the pressure exceeds 0.528 P_{th} are subsonic. Figure 3 shows that the profile designated by the circles has pressures greater than the reference pressures at all taps except tap A. Thus, the shock is said to be between taps A and B. The profile, designated by the triangles, was taken with the shock midway in the tap region. The four upstream taps A, B, C, and D are less than the reference pressure, and the four downstream taps E, F, G, and H are all greater than the reference pressure. We might say, therefore, that the shock is just upstream of tap E. The leading edge of the shock was actually located near the intersection between the profile denoted by the triangles and the supersonic distribution designated by the heavy line or between taps C and D. The indicated location is therefore in error by up to one tap location. The profile designated by the squares was taken with the shock downstream of the tap region and therefore coincides with the supersonic distribution line.

The logic necessary to implement the shock sensor is shown schematically in figure 4. The divider is required to produce a reference pressure that is a fraction of the throat total pressure. Each wall tap is compared to the reference pressure. If the tap pressure is greater than the reference pressure, the comparator output is on. And, if the tap pressure is less than the reference pressure, the comparator output is off. Thus, the outputs of all comparators connected to taps upstream of the normal shock are turned off and the outputs of all comparators connected to taps downstream of the shock are turned on.

Electronic Sensor

The electronic shock position sensor is shown schematically in figure 5. The wall static pressures are measured by means of eight strain gage type pressure transducers connected to the inlet cowl wall through short tubing. The frequency response of each pressure transducer and its connecting lines was flat within 0 to 1 decibel and had a phase lag of less than 8^{o} from 0 to 200 hertz. The comparators furnish an output when the individual transducer voltage exceeds the reference voltage. The comparator outputs perform two functions. The output voltages operated relays which switched on and off a row of panel lights in the control room. Also, the output voltages of all of the comparators were summed together in one analog summing amplifier to provide an electronic stepwise continuous signal proportional to the normal shock position. The reference voltage was generated by passing the output of another pressure transducer, measuring throat total pressure, through a voltage dividing potentiometer. The potentiometer was set so that the reference voltage equalled 0.528 times the throat total pressure.

Fluidic Sensor

The same basic logic scheme was used in the fluidic sensor as was used in the electronic sensor. However, the comparators were fluidic amplifiers which sensed the wall static pressure directly. A schematic diagram of the fluidic sensor is shown in figure 6. The fluidic sensor was self-contained in that the supply pressure was furnished by a total pressure probe in the inlet diffuser feeding through a dropping orifice. The reference pressure was generated by a total pressure probe in the inlet throat feeding through two dropping orifices to tunnel static pressure. The reference pressure can be adjusted up or down by changing the size of either of the orifices. The bottom orifice exhausts directly to tunnel static pressure. Not shown in the figure are the amplifier vents which exhausted to the tunnel static pressure through a suitably sized orifice.

The supply pressure orifice and amplifier vent orifice were sized so that the pressure ratio between the supply pressure and the vent pressure was less than two and the vent pressure never exceeded the reference pressure or input pressure.

The fluidic amplifiers were high input impedance, wall attachment monostable amplifiers designed by the U.S. Army's Harry Diamond Laboratories and are described in detail in reference 5. An outline of one of the amplifiers is shown in figure 7. A high input impedance is created in the amplifier by means of a bias slot between the supply port and the input pressure port. This is shown in figure 7(a). Since the supply pressure is higher than any other pressure in the amplifier, air always flows through the bias slot into the input pressure passage. When the input pressure is lower than the

reference pressure (fig. 7(b)) this flow exits the amplifier through the input port. The stream entrains air through the return slot creating a lower pressure region on the left side of the supply jet causing the supply jet to be deflected to output port O_1. When the input pressure is greater than the reference pressure (fig. 7(c)), flow reverses in the input pressure port and the bias flow is diverted through the return slot. A high pressure region is now created on the left side of the supply jet, causing it to be diverted through output port O_2.

The outputs of each amplifier were connected to a small pressure switch to provide an electrical output to the sensor. The switch outputs were connected to a row of panel lights in the control room. The switch outputs were also summed together using an analog summing amplifier to provide a stepwise continuous output signal proportional to normal shock position.

Direct-Connected Switches Sensor

The simplest of the three sensors tested consisted of a set of sensitive differential pressure switches as shown in figure 8. The low pressure port of each switch was connected to the reference pressure, and the high side of each switch was connected to one wall static pressure tap. If the wall static tap pressure exceeded the reference pressure the switch was turned on. The switch outputs were connected to a row of panel lights in the control room. The reference pressure was generated by means of two dropping orifices in a manner similar to that used to obtain the fluidic sensor reference pressure. The reference pressure was set at a value equal to 0.528 times the throat total pressure.

The switches, which were purchased as an inexpensive, off-the-shelf, commercial item, were designed to perform reliably with extremely small differential pressures, less than 0.012 newton per square centimeter. The switch bodies were made of fiber glass filled polycarbonate plastic and the diaphrams were of fluorocarbon plastic sheet.

EXPERIMENTAL RESULTS AND DISCUSSION

Apparatus

Inlet. - The three types of normal shock position sensors were tested in a two-dimensional, Mach 2.7 supersonic inlet installed in the Lewis 10- by 10-Foot Supersonic Wind Tunnel. The inlet, shown in figure 9, has two ducts separated by a collapsible ramp centerbody. The inlet was terminated with a choked orifice plate located between the cowl and the centerbody. Seventy percent of the supersonic area contraction occurs externally at the design Mach number of 2.7. The inlet has a performance bleed system

which consists of several rows of holes on the ramp, cowl, and sidewall surfaces. Bleed flow through the bleed is collected and ducted overboard.

An overboard bypass system is used for matching inlet and engine flow requirements. The bypass system consists of two slotted, sliding-plate doors in each duct. The doors were individually controllable by means of electro-hydraulic servomechanisms. The doors have unusually high response - 140 hertz bandwidth as shown in figure 10. The test peak-to-peak amplitude was 18 percent of full stroke. In this program the doors were used to vary the position of the normal shock in the inlet throat.

The dynamic responses of the inlet shock position and several other inlet pressures to overboard bypass airflow are reported in reference 6.

Sensor tap locations. - Two electronic sensors were installed in the inlet, one in the upper duct and one in the lower. The wall static pressure tap locations are shown in figure 11. As shown, the wall taps for the electronic sensor were located 8.64 centimeters off the inlet centerline. The fluidic sensor was located in the lower duct only with the taps 10.45 centimeters off the inlet centerline. And the direct switches were located in the upper duct only with the taps located 10.45 centimeters off the inlet centerline. The axial locations of the taps were the same for all four sensors and are labeled A to H.

Static Test Results

Procedure. - The steady-state performance of the sensors was determined by first positioning the shock at some location within the wall static pressure tap region. The output of each sensor was then read and compared to the actual shock location as determined by the wall static pressure profile. The pressure transducer outputs of the electronic sensor were used to determine the wall static pressure profiles for evaluating the fluidic and direct-connected switch sensor.

Electronic sensor. - The steady-state performance of the electronic shock position sensor is shown in figures 12 to 15. Figures 12 and 13 show the performance of the electronic sensor located in the lower duct for Mach 2.7 and 2.3, respectively, and figures 14 and 15 show the performance of the upper duct electronic sensor at Mach 2.7 and 2.3, respectively.

In figure 12(a) the steady-state performance is shown for the 0° angle-of-attack condition. The curves show the wall static pressure profile for three different shock positions. The chart beneath the graph indicates the condition of the output of the sensor for each of the three shock positions. It can be seen from this figure and in subsequent figures that the output associated with each wall static tap is on when that tap is of higher pressure than the reference value. In some cases the output is intermittent in which

case the light associated with that output flashes on and off. This is caused by fluctuations in the wall static pressures.

It should be noted that the pressure at tap A is always lower than that at tap B. Wall static pressure profiles taken before the total pressure probe was installed always showed tap A to be greater than tap B. It can therefore be concluded that the presence of the total pressure probe influenced the reading of the tap A.

In comparing the sensor output with the actual shock position it can be seen that the shock sensor output indicates the shock to be about two taps behind the actual shock position. The same trend is noted in figure 13. Figure 14, which shows the performance for the upper duct sensor, illustrates the effect of inlet angle of attack on the sensor accuracy. The upper duct, being on the leaward side of the flow, captures less flow, thus increasing the throat Mach number. This, in turn, causes the supersonic values of the cowl static pressures to be lower than in the lower duct, resulting in an output indication several taps downstream of the actual shock position.

The sensor used in these tests used only one reference voltage for comparison with each wall static pressure. As shown in figure 5, this reference voltage is obtained by using a voltage dividing circuit; in this case a potentiometer was used. If an additional voltage dividing circuit were used with each wall static pressure tap, different reference voltages corresponding to different fractions of the reference pressure could be used on each wall static tap. These individual reference voltages could then be set so that the reference voltage for each tap is a small amount greater than the supersonic value corresponding to that tap. If such a circuit were used, indication of shock position within one or two taps could be obtained.

Off-design Mach number operation, does not adversely affect the accuracy of the sensor as shown in figures 13 and 15. Wall static pressure profiles taken with the ramp at off-design positions show that the pressure profiles were about the same as they were when the ramp was at the design position. Therefore, off-design ramp position test results will not be shown.

Fluidic sensor. - The steady-state performance of the fluidic sensor is shown in figures 16 and 17. Figure 16 shows the performance at design Mach number 2.7. It should also be noted here that the pressure values shown in the plotted curves of figures 12 to 18 were actually read from the transducers used for the electronic shock sensor. As stated previously, the throat total pressure probe used to obtain reference pressures influenced the reading of the electronic sensor tap A causing it to read low.

The most pronounced difference between these results and the results of the electronic sensor tests is that the reference pressure varied as a function of supply pressure, and since the supply pressure probe was located in the subsonic diffuser, the supply pressure varied with shock position. The net result of this effect was that the reference pressure dropped as the shock moved downstream in the duct. The dependency of the reference pressure on supply pressure is caused by the characteristics of

the fluidic amplifiers themselves. The input impedance of the reference port is proportional to the amplifier supply pressure. As the supply pressure drops, the impedance of each amplifier's reference port drops, allowing more flow to be taken from between the two dropping orifices which furnish the reference pressure source. Taking more flow from between the orifices causes the reference pressure to drop. In several cases the reference pressure actually dropped lower than the pressure at tap A, causing the A output to come on. This is shown in figures 16(a) and 17(a) and (b).

The performance of the sensor probably could be improved by taking the amplifier supply pressure from the same Pitot tube as the reference pressure supply in the inlet throat.

Generally, the sensor indicated the shock position within two taps downstream of the actual shock position.

Direct-connected switches sensor. - The steady-state performance of the direct switches sensor is shown in figure 18. These results show that the output would be accurate to within one or two taps if the reference pressure were set to a value slightly greater than the highest supersonic wall static tap pressure.

After approximately two runs the switches started to leak through the diaphrams. The switches are rated for over one million cycles before failure; however, with the high frequency noise present in the inlet, one million cycles can be accumulated in a few hours of run time.

Dynamic Test Results

Procedure. - The responses of all three shock position sensors to normal shock motions were obtained for frequencies out to 80 hertz. The shock motion was induced by driving the bypass doors in a sinusoidal manner. The output of the shock position sensors were displayed for each frequency directly on an oscilloscope screen. The range of the shock motion was constantly observed during the test by monitoring the pressures of each individual wall static pressure on a light beam oscillograph.

Electronic sensor. - Figure 19 shows the outputs of both the electronic sensor and the fluidic sensor on the same oscilloscope photo at frequencies from 1 to 80 hertz. The upper trace in each case is the output of the electronic sensor and the lower trace is the output of the fluidic sensor.

At 10 hertz the electronic sensor was indicating that all nine levels of output were being actuated. However, as has already been shown in the steady-state performance discussion, the shock must be some distance beyond tap A before all nine levels can be in the on condition. At 20 hertz the A output is no longer being turned on. At 80 hertz only the outputs downstream of tap E including E are being turned on for every cycle.

Fluidic sensor. - It can be seen in figure 19(a) that only eight levels of output are on when the shock is far enough upstream to turn on all nine levels of the electronic sensor. This is due to the reference pressure of the fluidic sensor varying with the shock position as was shown in the discussion of the steady-state performance. With the shock upstream the fluidic sensor reference pressure was considerably greater than the desired pressure of 0.528 times the throat total pressure. It is therefore concluded that the shock was never far enough upstream to turn the A output on. At 40 hertz the B output also drops out. For the remainder of the test, out to 80 hertz, the fluidic sensor indicated the remaining seven levels of output.

Direct-connected switches sensor. - Figure 20 shows a comparison of the dynamic performance of the sensor using the direct-connected switches with that of the upper duct electronic sensor. The upper trace shows the output of the electronic sensor, and the lower trace shows the output of the direct switches sensor.

Even at 1 hertz, the sensor using the direct switches only had six output levels in the on condition when the shock was far enough upstream to activate all nine levels of the electronic sensor. At the time of this test the switches had been installed in the inlet for several runs and past experience with the switches indicates that the switches were leaking. This would cause the reference pressure to vary with the shock position. This caused the reference pressure to be higher than it was originally set, when the shock was in the most upstream position resulting in the loss of output levels as indicated. Erratic operation of the switches at higher frequencies indicates probable bouncing of the switch contacts.

It should be noted that the dynamic performance of the upper duct electronic sensor, shown in figure 20, appears to be better than the dynamic performance of the lower duct electronic sensor, shown in figure 19. At least seven levels are actuated at 80 hertz. Improved performance is probably a result of operating at a mean shock position upstream of the lower duct tests.

SUMMARY OF RESULTS

This report presents the results of tests conducted on three normal shock position sensors designed for use in a mixed-compression supersonic inlet. All three sensors determine shock position by comparing the wall static pressures, in the vicinity of the inlet throat, with a reference pressure.

Electronic sensor. - Results of static tests on the electronic sensor show that the sensor in the lower duct indicated the shock position within two taps downstream of the actual shock. The sensor in the upper duct, however, indicated the shock position several taps downstream of the actual position when the inlet was at angle of attack. As

pointed out in the Static Test Results section, this condition is due to the decreased capture airflow in the upper duct when the inlet is at a positive angle of attack.

Dynamic tests on the electronic sensor show that the output omits some levels at frequencies beyond 20 hertz as the shock is moved over the taps by oscillating the bypass doors in a sinusoidal manner. It is felt that this is due to the reference pressure being set too high and not due to a lack of response in the sensor hardware.

Both the steady-state and dynamic performance of the sensor could be improved by providing different reference voltages for each pressure tap. It is recommended that future electronic sensor circuitry be revised to include this improvement.

Fluidic sensor. - Generally, for static tests, the fluidic sensor indicated the shock position two taps downstream of the correct shock position. Improved operation could probably be obtained by taking the amplifier supply pressure from the same Pitot tube as the reference pressure supply so that the reference pressure will remain constant. Dynamic performance of the fluidic sensor was satisfactory over the frequency range of 1 to 80 hertz with only one output level being dropped out above 40 hertz.

Direct-connected switches sensor. - Although the steady-state accuracy of the switches was as good as the electronic and fluidic sensors, the lifetime of the switches was quite short. Improved switches with metallic diaphrams would be required before a sensor could be expected to operate more than just a few hours. The frequency response of the switches is poor compared to the other two sensors.

The switches used with the fluidic sensor were identical to those used in the direct-connected switches sensor. These switches also leaked. However, since the switches were not connected directly to the reference pressure, as were the direct connected switches, the leakage did not affect the reference pressure.

Lewis Research Center,
National Aeronautics and Space Administration,
Cleveland, Ohio, November 17, 1972,
501-24.

REFERENCES

1. Griffin, William S.: Design and Performance of a Flueric Shock Position Sensor for a Mixed-Compression Supersonic Inlet. NASA TM X-1733, 1969.
2. Cole, Gary L.; Neiner, George H.; and Crosby, Michael J.: Design and Performance of a Digital Electronic Normal Shock Position Sensor for Mixed-Compression Inlets. NASA TN D-5606, 1969.

3. Dustin, Miles O.; Cole, Gary L.; and Wallhagen, Robert E.: Determination of Normal-Shock Position in a Mixed-Compression Supersonic Inlet. NASA TM X-2397, 1971.

4. Johnson, Elmer G.: Control Apparatus. Patent No. 3, 460, 554, United States, Aug. 1969.

5. Holmes, Allen B.; Gehman, Stacy E.; Egolf, David; and Lewellan, Michael: Flueric Normal Shock Sensor. Rep. TM-69-9, Harry Diamond Lab. (NASA CR-107688), Apr. 1969.

6. Baumbick, Robert J.; Neiner, George H.; and Cole, Gary L.: Experimental Dynamic Response of a Two-Dimensional, Mach 2.7, Mixed-Compression Inlet. NASA TN D-6957, 1972.

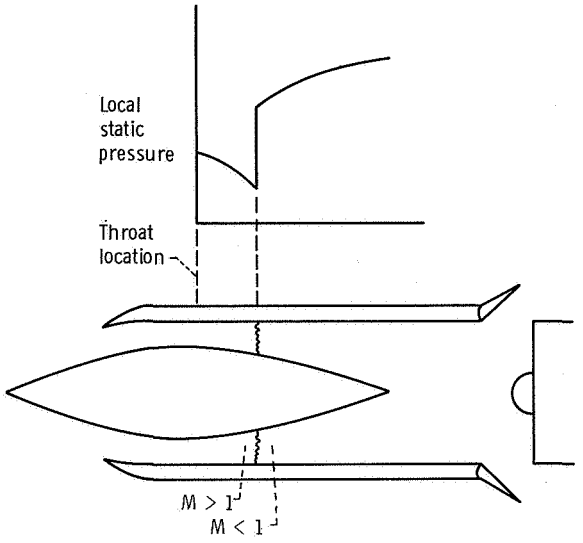

Figure 1. - Ideal static pressure profile in vicinity of normal shock.

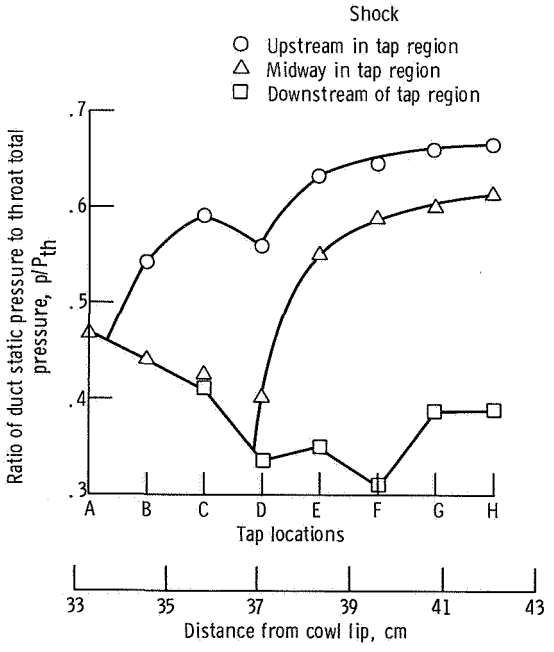

Figure 2. - Typical inlet cowl static-pressure profiles with normal shock in three locations.

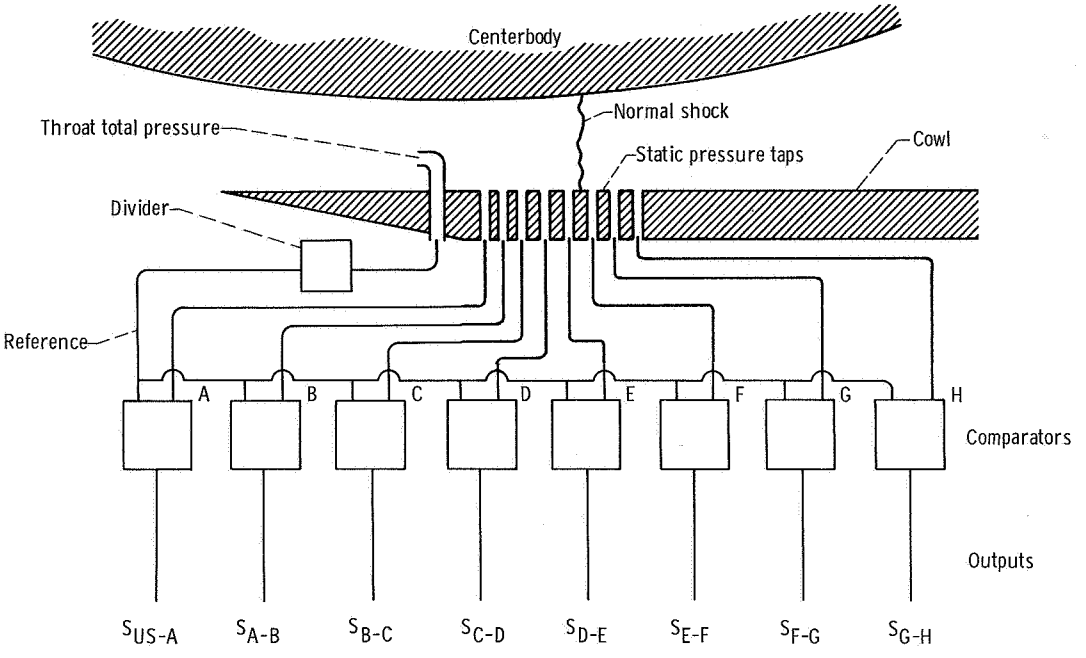

Figure 4. - Schematic representation of normal shock position sensor logic.

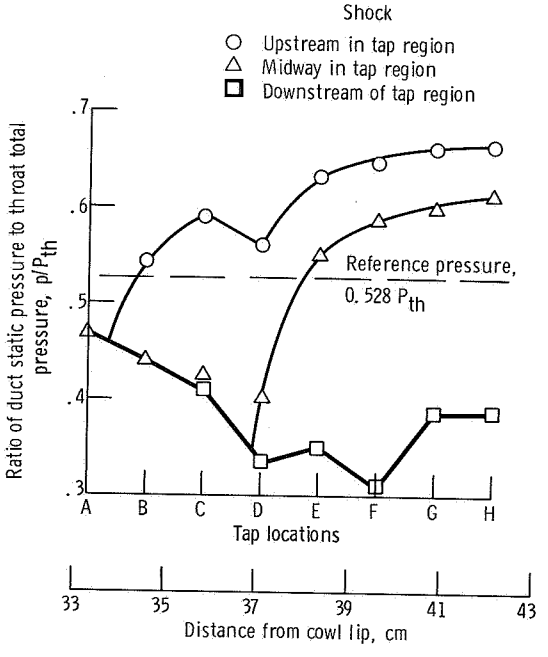

Figure 3. - Illustration of principle of operation of shock position sensors using typical inlet cowl static pressure profiles.

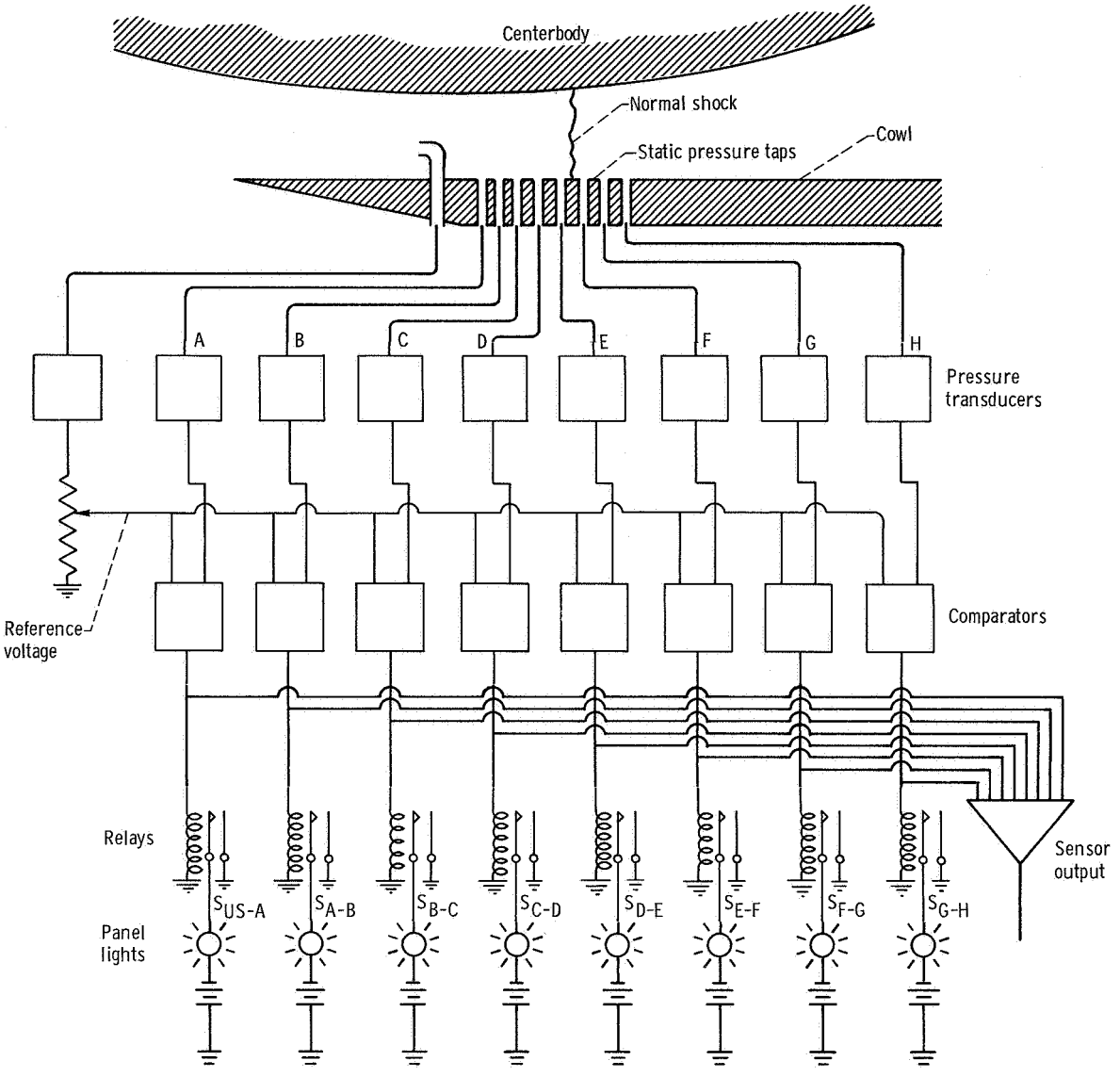

Figure 5. - Schematic representation of electronic shock position sensor.

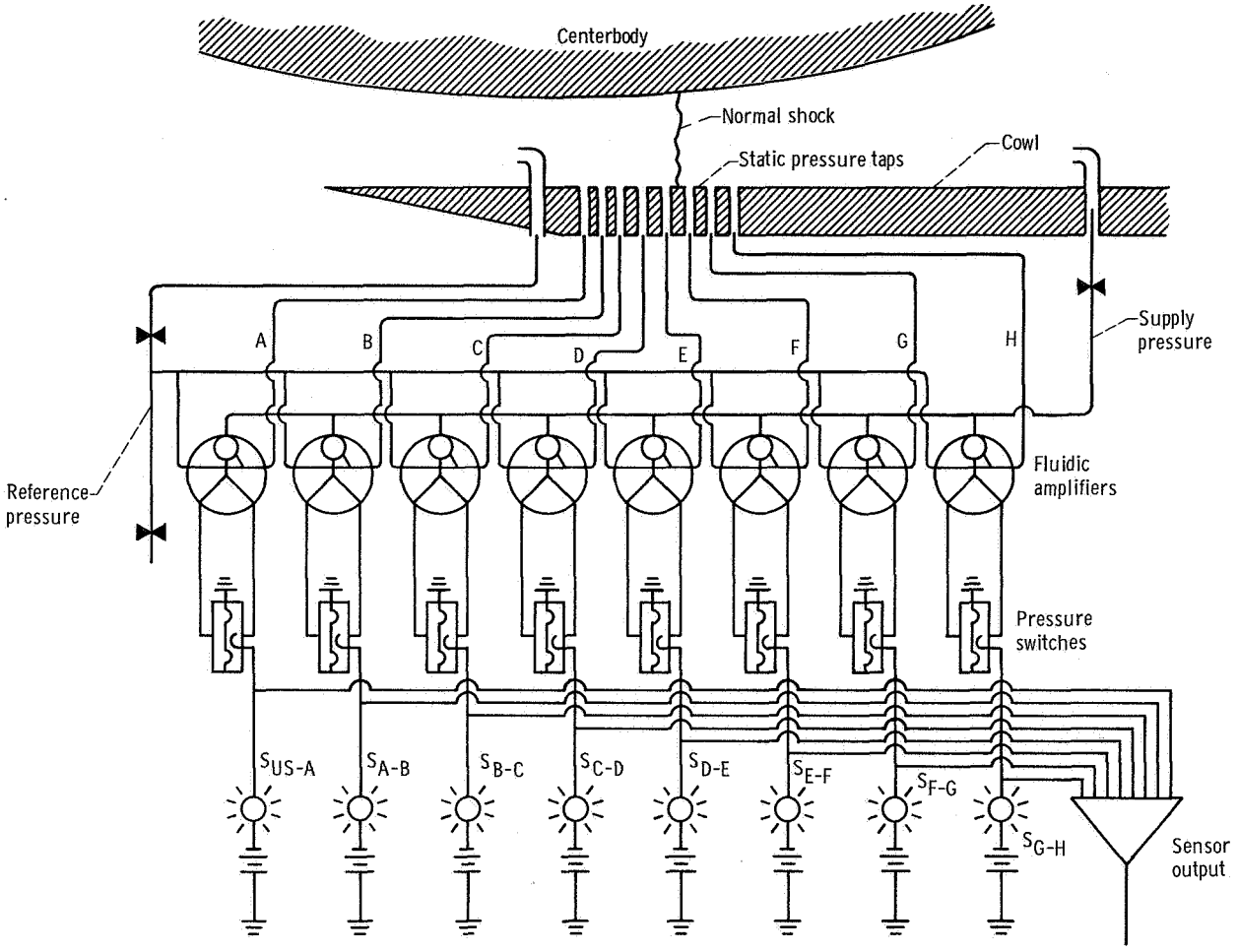

Figure 6. - Schematic representation of fluidic shock position sensor.

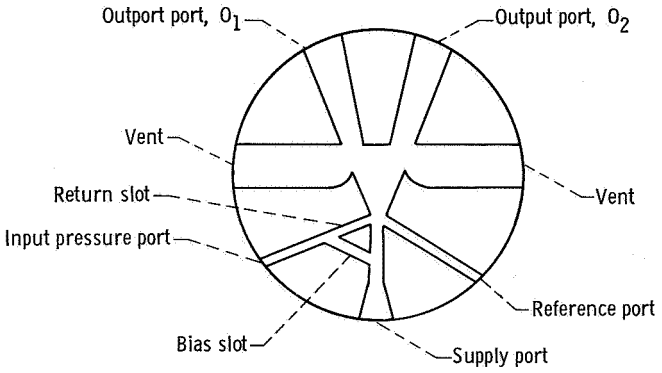

(a) Amplifier schematic.

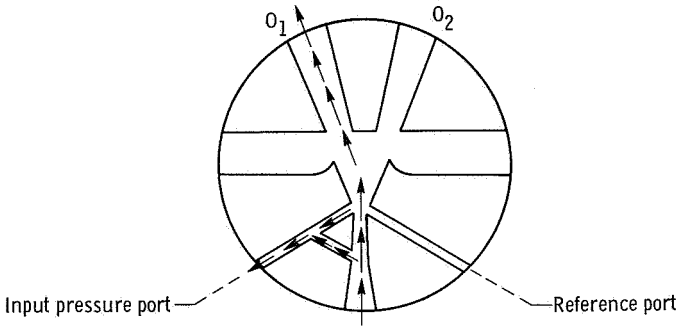

(b) Reference greater than input.

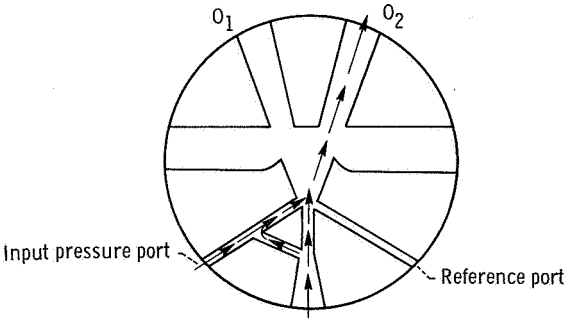

(c) Reference less than input.

Figure 7. - High impedance fluidic amplifier used in fluidic shock position sensor.

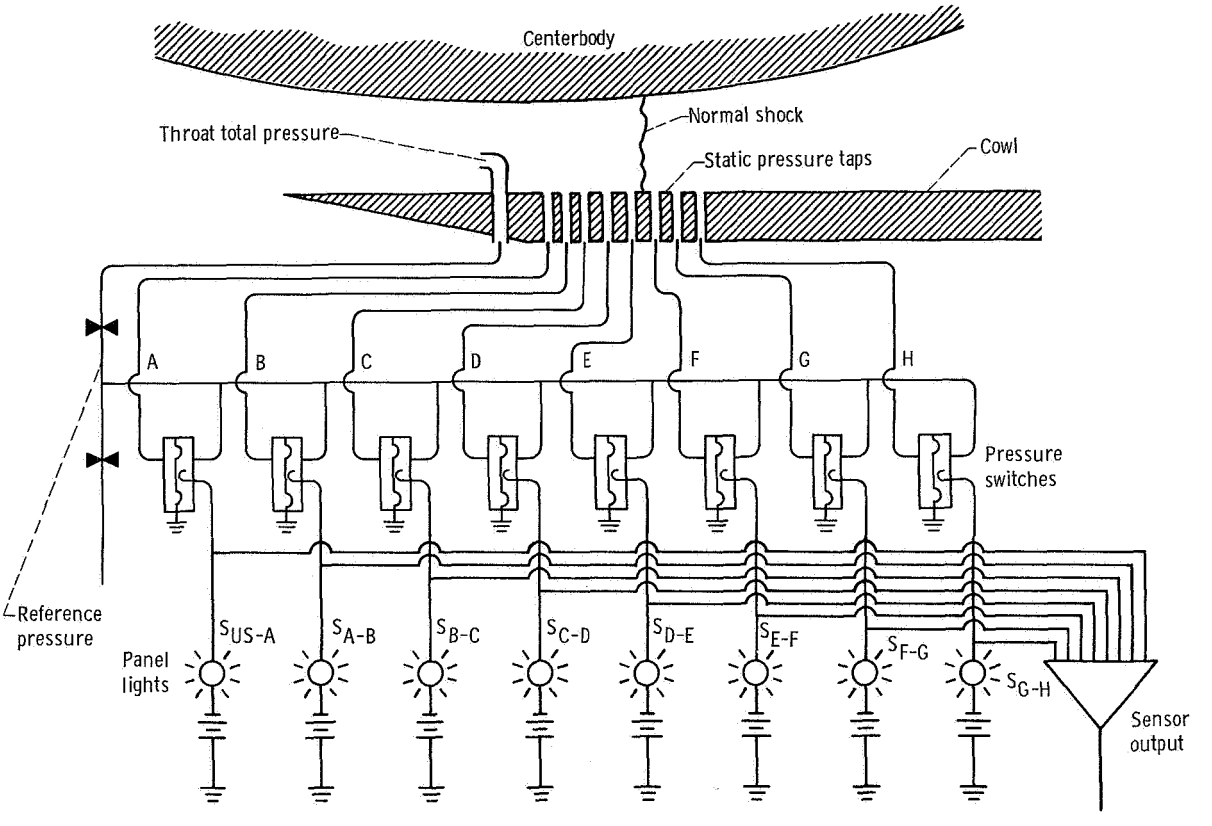

Figure 8. - Schematic representation of shock position sensor using direct-connected switches.

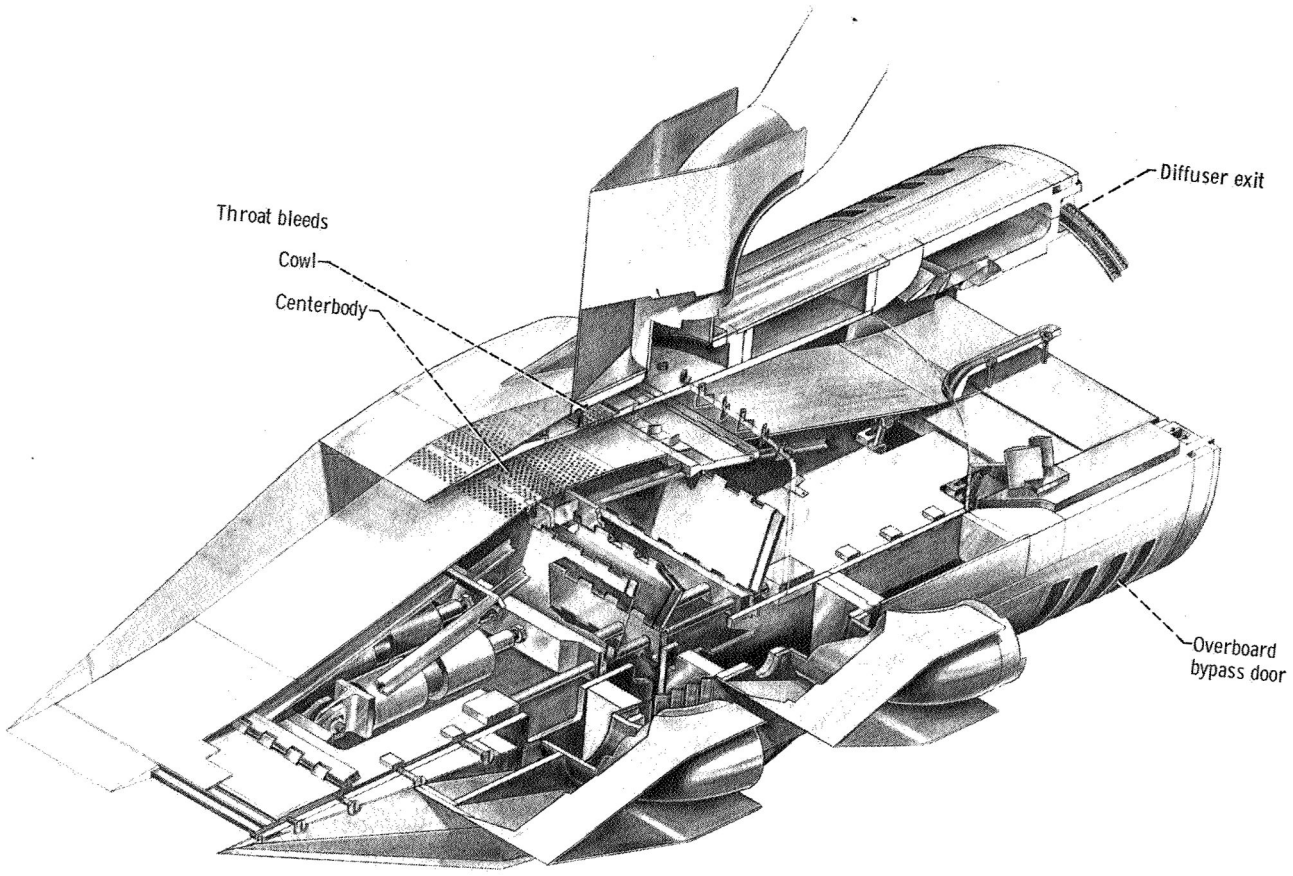

Figure 9. - Isometric view of inlet.

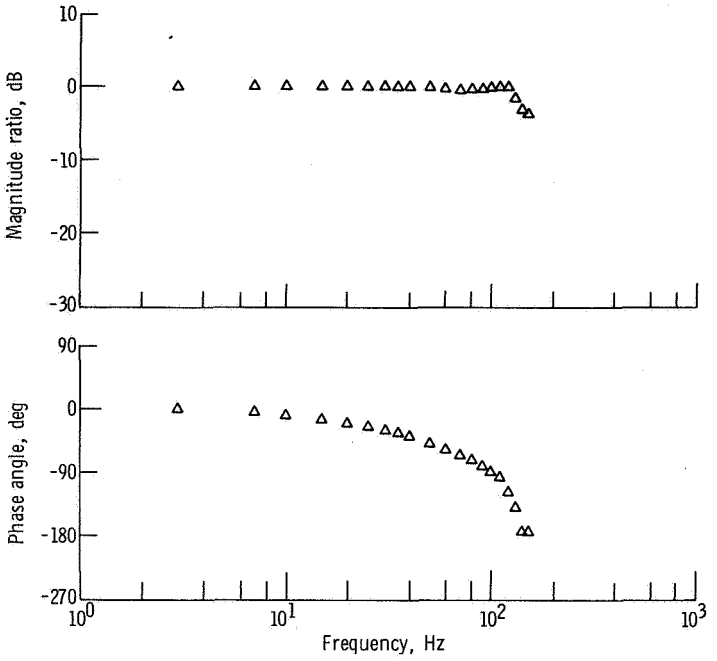

Figure 10. - Response of overboard bypass door to sinusoidal input voltage. Peak- to-peak movement of 0.42 centimeter (16 percent of maximum door travel).

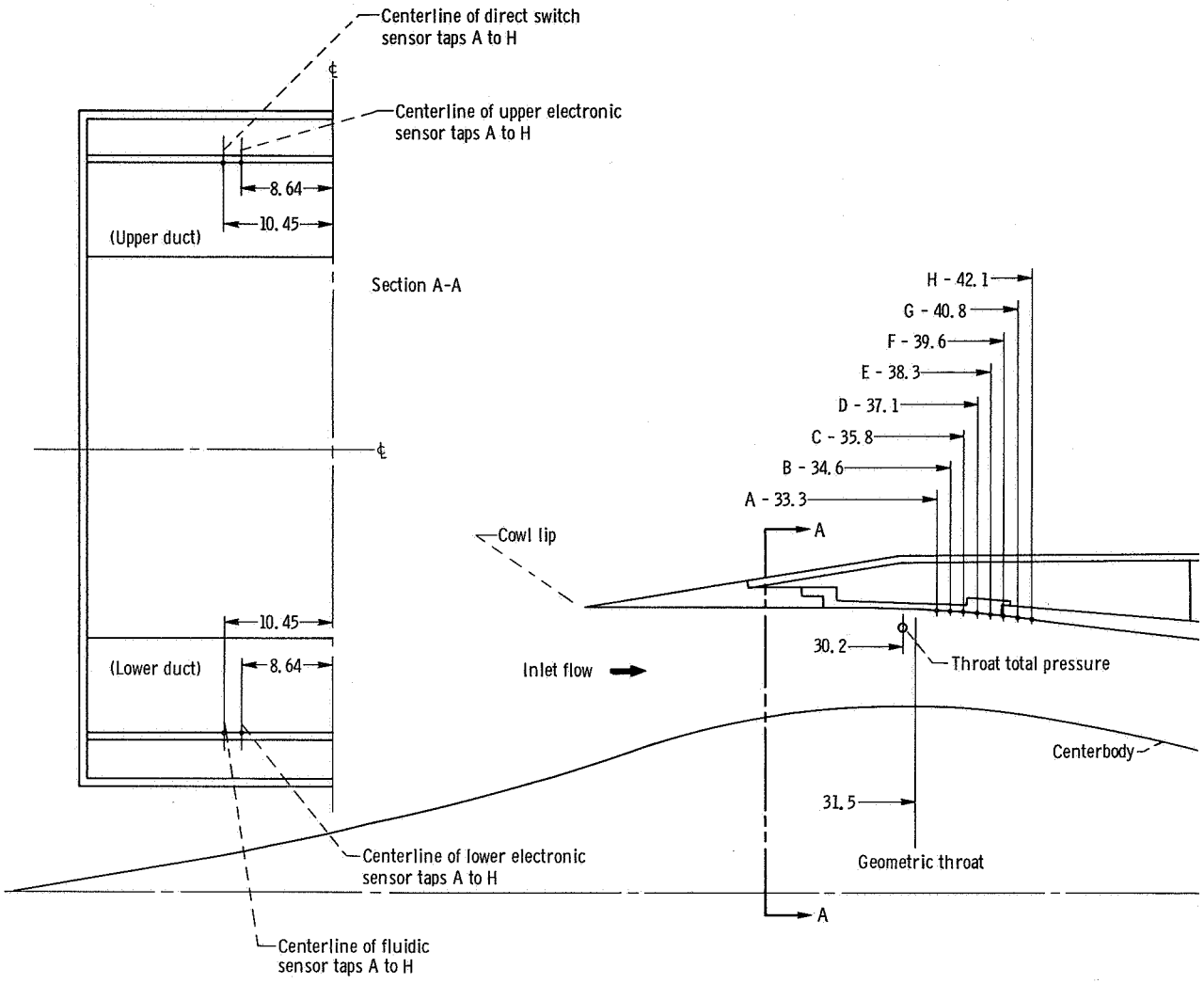

Figure 11. - Inlet normal shock sensor tap locations. (Dimensions in centimeters from cowl lip.)

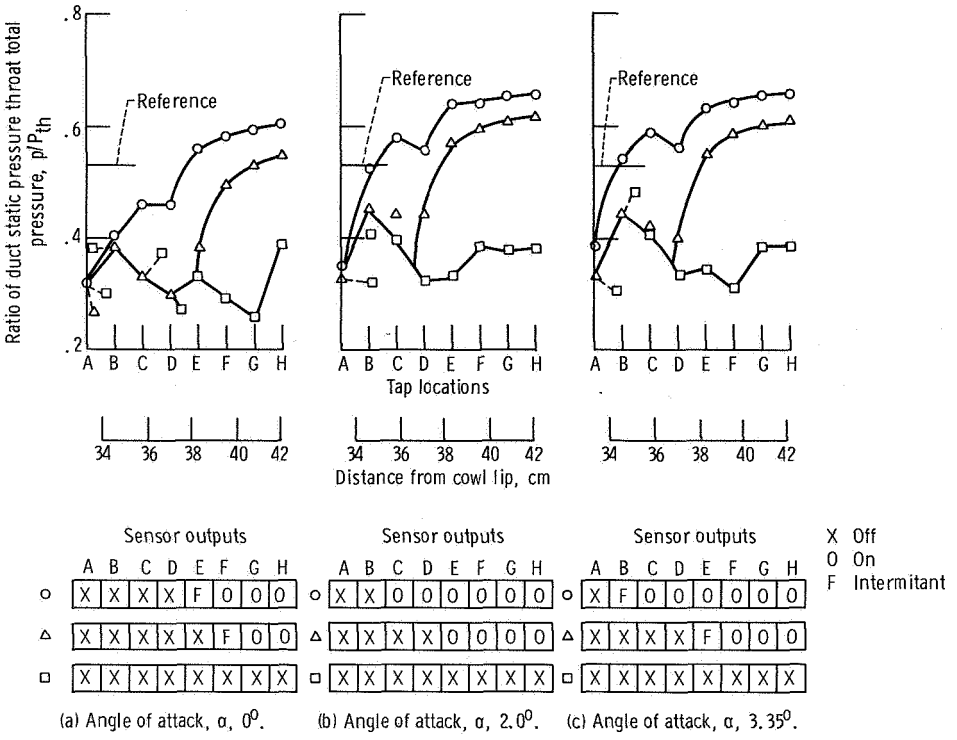

Figure 12. - Comparison of lower duct electronic shock sensor output with actual normal shock position as determined by wall static pressure profiles. Mach number, 2.7.

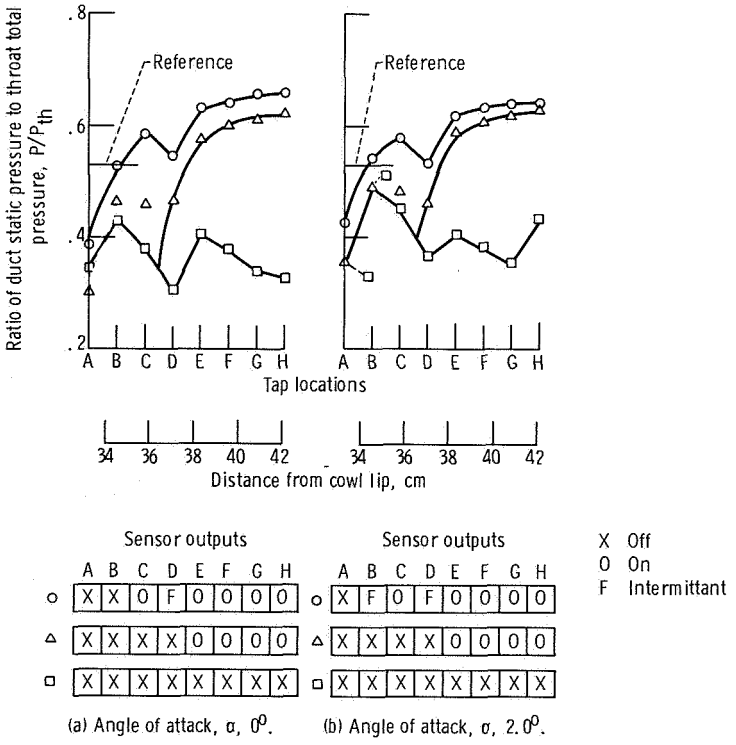

Figure 13. - Comparison of lower duct electronic shock sensor output with actual normal shock position as determined by wall static pressure profiles. Mach number, 2.3.

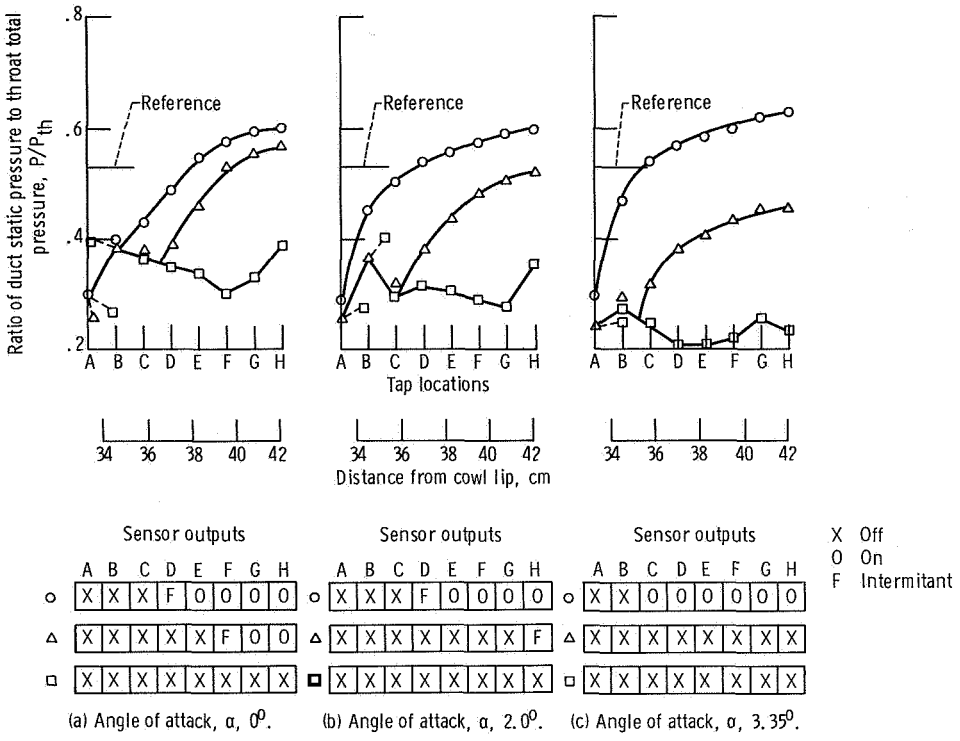

Figure 14. - Comparison of upper duct electronic shock sensor output with actual normal shock position as determined by wall static pressure profiles. Mach number, 2.7.

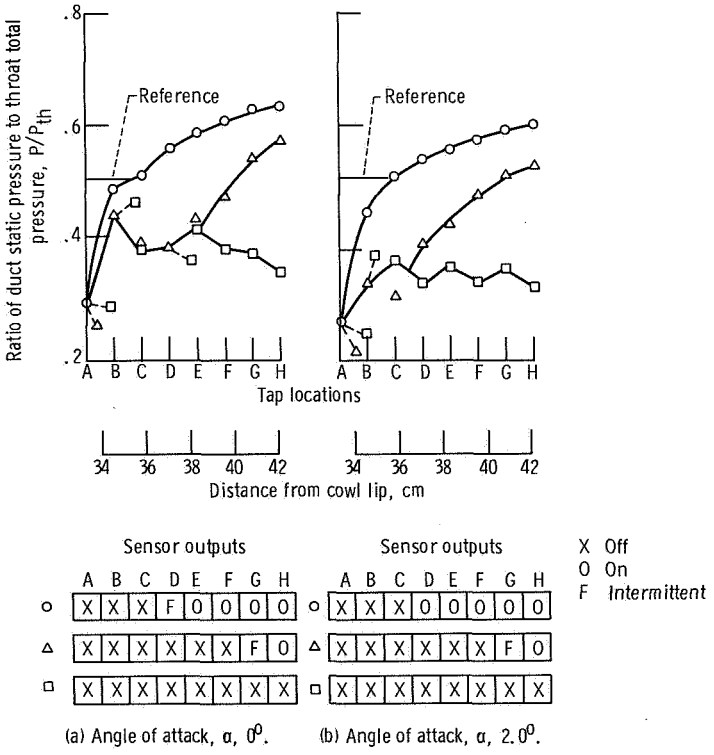

Figure 15. - Comparison of upper duct electronic shock sensor with actual normal shock position as determined by wall static pressure profiles. Mach number, 2.3.

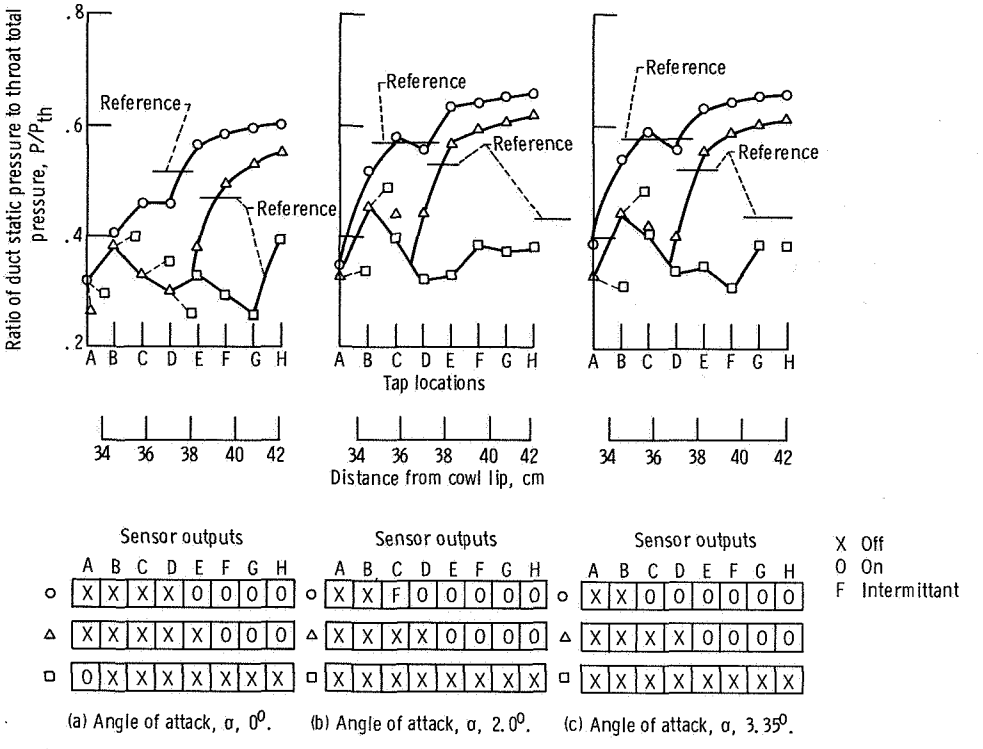

Figure 16. - Comparison of fluidic shock sensor output with actual normal shock position as determined by wall static pressure profiles. Mach number, 2.7; sensor in lower duct.

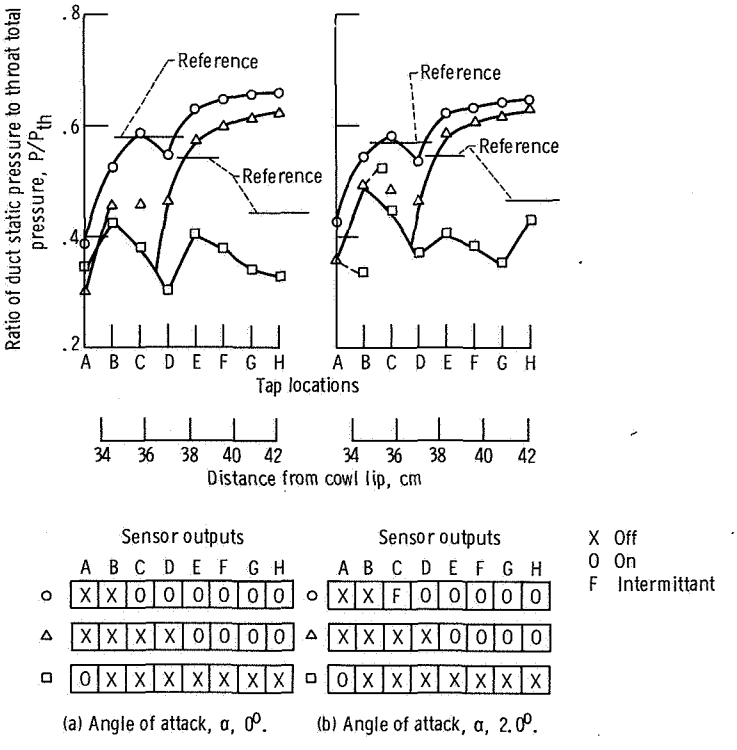

Figure 17. - Comparison of fluidic shock sensor output with actual normal shock position as determined by wall static pressure profiles. Mach number, 2.3; sensor in lower duct.

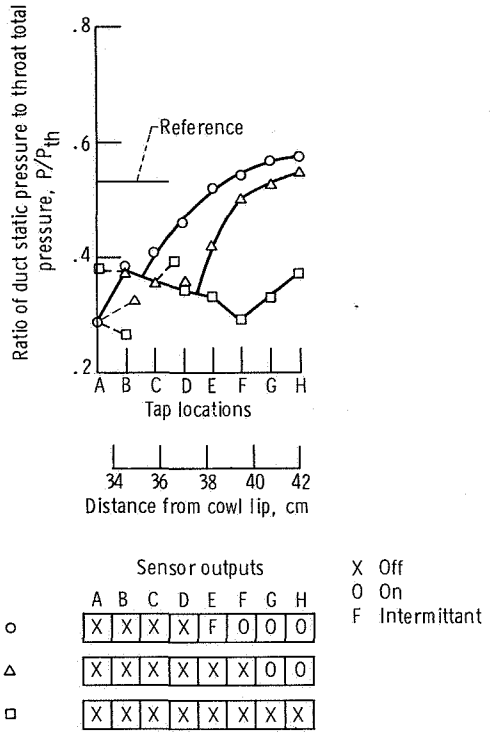

Figure 18. - Comparison of direct-switches shock sensor output with actual normal shock position as determined by wall static pressure profiles. Mach number, 2.7; angle of attack, 0^{0}; sensor in upper duct.

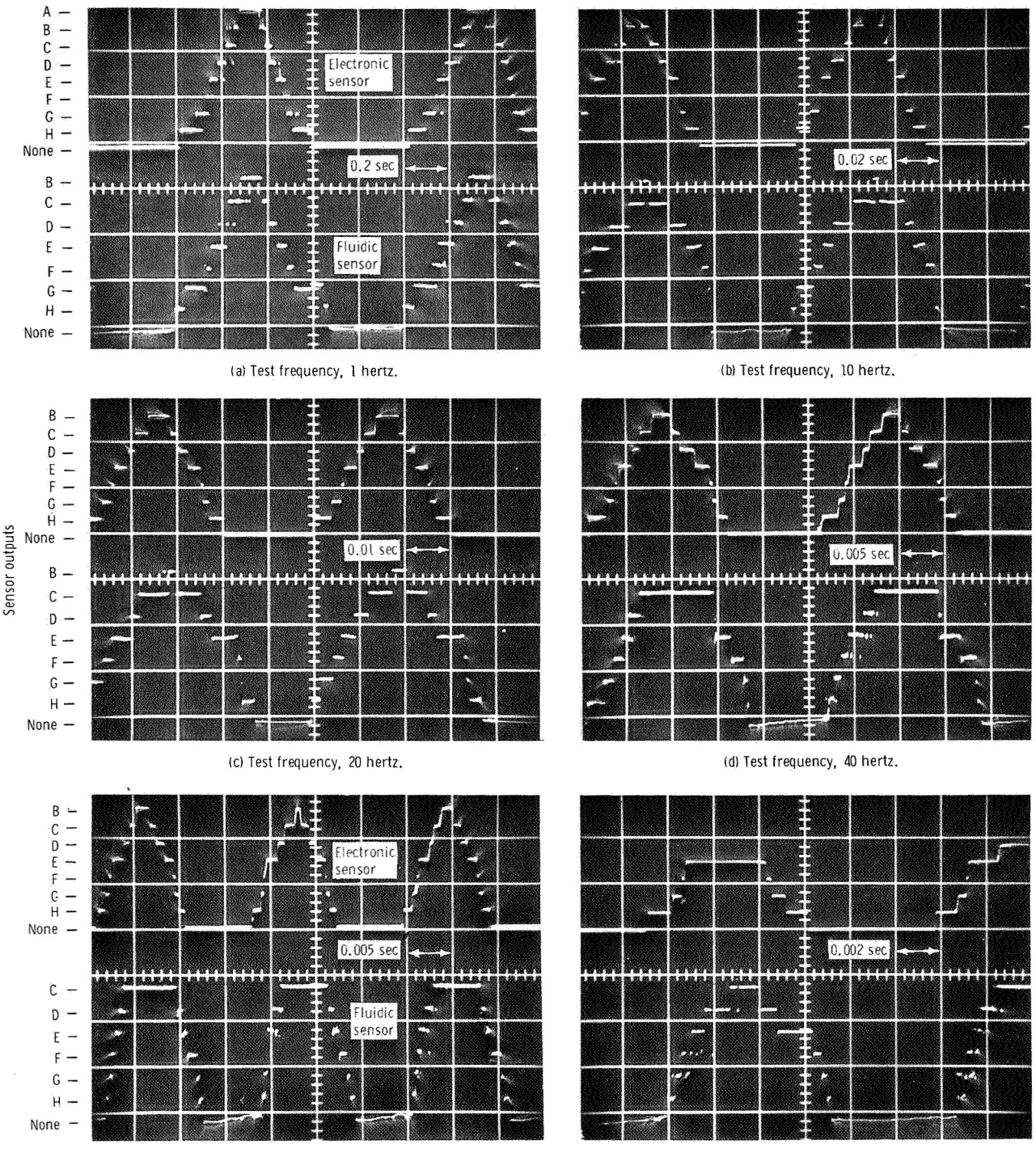

(a) Test frequency, 1 hertz.

(b) Test frequency, 10 hertz.

(c) Test frequency, 20 hertz.

(d) Test frequency, 40 hertz.

(e) Test frequency, 60 hertz.

(f) Test frequency, 80 hertz.

Figure 19. - Dynamic response of lower duct electronic and fluidic shock position sensors.

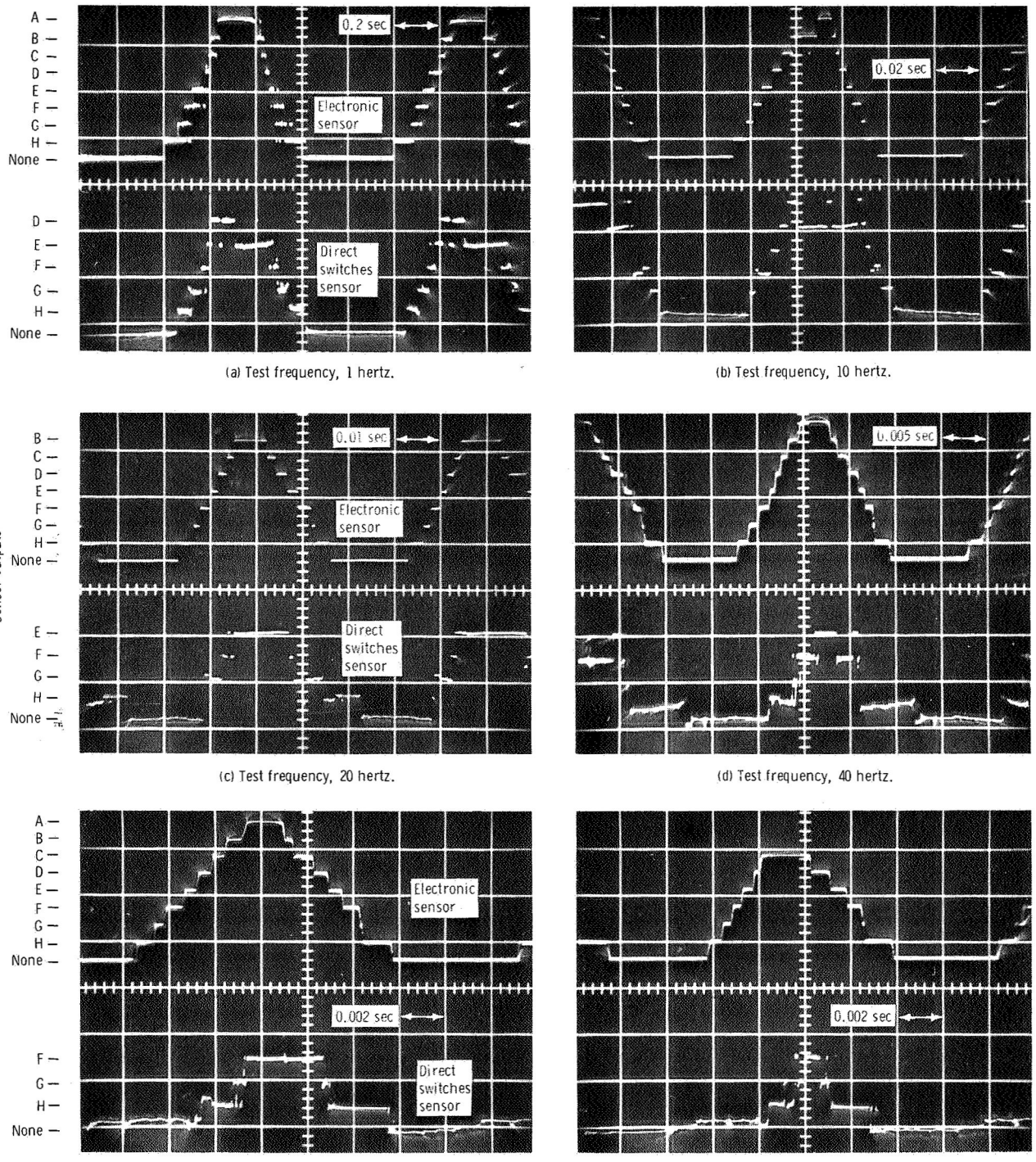

(a) Test frequency, 1 hertz.

(b) Test frequency, 10 hertz.

(c) Test frequency, 20 hertz.

(d) Test frequency, 40 hertz.

(e) Test frequency, 60 hertz.

(f) Test frequency, 80 hertz.

Figure 20. - Dynamic response of upper duct electronic and direct-switches shock position sensors.

1. Report No.	2. Government Accession No.	3. Recipient's Catalog No.
NASA TM X-2739		

4. Title and Subtitle	5. Report Date
PERFORMANCE COMPARISON OF THREE NORMAL-SHOCK POSITION SENSORS FOR MIXED-COMPRESSION INLETS	March 1973
	6. Performing Organization Code
7. Author(s)	8. Performing Organization Report No.
Miles O. Dustin and Gary L. Cole	E-7197
	10. Work Unit No.
9. Performing Organization Name and Address	501-24
Lewis Research Center National Aeronautics and Space Administration Cleveland, Ohio 44135	11. Contract or Grant No.
	13. Type of Report and Period Covered
12. Sponsoring Agency Name and Address	Technical Memorandum
National Aeronautics and Space Administration Washington, D.C. 20546	14. Sponsoring Agency Code

15. Supplementary Notes

16. Abstract

The performance of three types of normal shock position sensors for supersonic inlets is described. All three sensors determined the shock position from the presence of the large pressure gradient at the normal shock location. The logic means for the three sensors were (1) electronic, using pressure transducers, (2) fluidic, and (3) direct-coupled pressure switches. The sensors were evaluated in a two-dimensional, Mach 2.7, supersonic inlet having 30-percent internal supersonic area contraction. Both dynamic (from 1 to 80 Hz) and static tests were conducted.

17. Key Words (Suggested by Author(s))

Normal shock
Supersonic
Inlet
Sensor
Mixed compression

18. Distribution Statement

Unclassified - unlimited

19. Security Classif. (of this report)	20. Security Classif. (of this page)	21. No. of Pages	22. Price*
Unclassified	Unclassified	28	$3.00

* For sale by the National Technical Information Service, Springfield, Virginia 22151

NATIONAL AERONAUTICS AND SPACE ADMINISTRATION
WASHINGTON, D.C. 20546

OFFICIAL BUSINESS
PENALTY FOR PRIVATE USE $300

SPECIAL FOURTH-CLASS RATE
BOOK

POSTAGE AND FEES PAID
NATIONAL AERONAUTICS AND
SPACE ADMINISTRATION
451

U.S. MAIL

POSTMASTER: If Undeliverable (Section 158
Postal Manual) Do Not Return

"The aeronautical and space activities of the United States shall be conducted so as to contribute . . . to the expansion of human knowledge of phenomena in the atmosphere and space. The Administration shall provide for the widest practicable and appropriate dissemination of information concerning its activities and the results thereof."

—NATIONAL AERONAUTICS AND SPACE ACT OF 1958

NASA SCIENTIFIC AND TECHNICAL PUBLICATIONS

TECHNICAL REPORTS: Scientific and technical information considered important, complete, and a lasting contribution to existing knowledge.

TECHNICAL NOTES: Information less broad in scope but nevertheless of importance as a contribution to existing knowledge.

TECHNICAL MEMORANDUMS: Information receiving limited distribution because of preliminary data, security classification, or other reasons. Also includes conference proceedings with either limited or unlimited distribution.

CONTRACTOR REPORTS: Scientific and technical information generated under a NASA contract or grant and considered an important contribution to existing knowledge.

TECHNICAL TRANSLATIONS: Information published in a foreign language considered to merit NASA distribution in English.

SPECIAL PUBLICATIONS: Information derived from or of value to NASA activities. Publications include final reports of major projects, monographs, data compilations, handbooks, sourcebooks, and special bibliographies.

TECHNOLOGY UTILIZATION PUBLICATIONS: Information on technology used by NASA that may be of particular interest in commercial and other non-aerospace applications. Publications include Tech Briefs, Technology Utilization Reports and Technology Surveys.

Details on the availability of these publications may be obtained from:

SCIENTIFIC AND TECHNICAL INFORMATION OFFICE

NATIONAL AERONAUTICS AND SPACE ADMINISTRATION

Washington, D.C. 20546